# CFD SIMULATION OF 3-D FLOW FIELD OVER CLEAN AND LOADED WING

By

MUHAMAD IMRAN BIN JALALUDDIN

FINAL PROJECT REPORT

Submitted to the Mechanical Engineering Programme
in Partial Fulfillment of the Requirements
for the Degree
Bachelor of Engineering (Hons)
(Mechanical Engineering)

Universiti Teknologi Petronas

Bandar Seri Iskandar

31750 Tronoh

Perak Darul Ridzuan

# CERTIFICATION OF APPROVAL

**CFD SIMULATION OF 3-D FLOW FIELD OVER CLEAN AND LOADED WING**

by

Muhamad Imran bin Jalaluddin

A project dissertation submitted to the
Mechanical Engineering Programme
Universiti Teknologi PETRONAS
in partial fulfilment of the requirement for the
Bachelor of Engineering (Hons)
(Mechanical Engineering)

Approved:

_____

Assoc. Prof Dr. Hussain Al-Kayiem

Project Supervisor

UNIVERSITI TEKNOLOGI PETRONAS

TRONOH, PERAK

June or December 2014

# CERTIFICATION OF ORIGINALITY

This is to certify that I am responsible for the work submitted in this project, that the original work is my own except as specified in the references and acknowledgements, and that the original work contained herein have not been undertaken or done by unspecified sources or persons.

_____

MUHAMAD IMRAN BIN JALALUDDIN

# ABSTRACT

The phenomenon of flow separation have long been a concern in the aviation field as it could cause many aviation issues such as aircraft stalling during take-off or landing which could lead to airplane crashes and fatality. This problem can become more severe in the high speed fighter jets. So far, very little have been reported on the on the visualization and analysis of the flow fields interaction of wing with load, such as drop tank or missile. This project aims to investigate the effect of airfoil configuration towards the occurrence of flow separation. The effect clean and loaded airplane wings or airfoils at several angle of attacks towards the severity of the flow separation was investigated. Furthermore, the amount of lift and drag force when the clean and loaded wing subjected to air flow at different angle of attack were also predicted. NACA 4412 airfoil was selected for this study via computational fluid dynamics (CFD) simulation in order to study the behavior of flow field over clean and loaded airfoils at angle of attack (AOA) of 0, 15, 17.5 and 20 degrees. Based on the initial simulation conducted upon clean and loaded airfoil at 0 degree angle of attack the pressure on the surface of the airfoil was predicted and presented via pressure contour, velocity magnitude as well as the lift and drag force that acts upon the scaled down computational solid model of the NACA airfoil. Next step is the study regarding this topic with greater detail at the other angle of attack.

# ACKNOWLEDGEMENTS

First and foremost, I would like to express my utmost humble gratitude and all the praises to ALLAH for His blessing and guidance in order for me to complete this Final Year Project entitled 'CFD Simulation of 3-D Flow Field over Clean and Loaded Wing' throughout the duration of Final Year Project I and Final Year Project II.

The completion of this project would not have been possible without endless support from those who are involved either directly or indirectly in this report. Furthermore, I would like to express my gratitude to my supervisor, Assoc. Prof Dr. Hussain Al-Kayiem for taking his time to assist me in completingx my final year project as well as for all the valuable input and knowledge that he have gave me.

I would also like to thank Mr. Andrew D'Onofrio and Mr. Javed Akbar Khan Niazi for their collaboration in this research project. All their inputs, support, and sharing of information have enabled me to undertake this project more efficiently as well as gain new knowledge.

Lastly, I would like to express my biggest thanks to my parent, who always pray for my best and always support me whenever I faced obstacles throughout completing of this final year project. I surely hopes that the outcome of this project may benefit to others as well.

Thank you.

# TABLE OF CONTENTS

# LIST OF FIGURES

## LIST OF TABLES

# CHAPTER 1

# INTRODUCTION

## 1.1 BACKGROUND STUDY

According to McGuigan (2014), an airfoil is a device that is capable to provide lift to an aircraft due to its design whereby the shape of the top is designed so that when air passes over the airfoil, the air speeds up hence decreasing the air pressure in that region according to Bernoulli's principle. Air below the airfoil is not affected, so its speed is the same as it was when it first contacted the airfoil. Air with a higher pressure tends to move towards air with a lower pressure, and as a result of the difference in pressure causes force to be exerted beneath the airfoil hence generating lift.

However, according to Fitzpatrick (2012), at high angle of attack flow separation could occur whereby resultant pressure force on the upper surface of the obstacle (airfoil) is equal and opposite to that on the underside of the obstacle hence causing the pressure distribution to gives rise to zero net drag acting on the obstacle. As a result, this situation could cause an aircraft to stall mid-flight. This situation is undesirable in the field of aeronautics.

Therefore, the purpose of this project would be to investigate the characteristics of fluid flow on airfoils with and without a load under the airfoil via computational simulation to determine whether phenomenon such as flow separation do occur under the given circumstances of this project such as the presence of load under the airfoil.

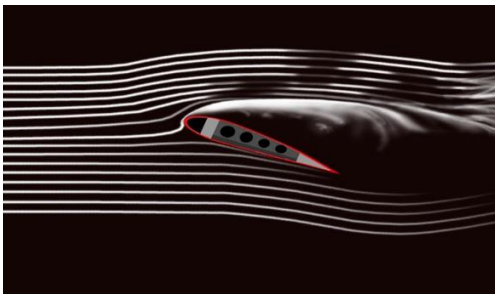

*Figure 1: Flow separation that occur on an airfoil*

## 1.2 PROBLEM STATEMENT

At high angle of attack, flow separation could occur whereby the fluid flow will be detached from the surface of the airfoil hence causing the formation of vortex or eddies. This phenomenon will then result in an increase of drag or worse will cause an object such as aircraft to stall mid-flight which is undesirable. Another factor that may either contribute to the separation of airflow, or worsen it is the presence of a load under the airfoil. Therefore, the project is intended to investigate the effect of presence of load under an airfoil towards the characteristics of airflow.

## 1.3 OBJECTIVE

1. To model and simulate the air flow over NACA 4412 airfoil in clean and loaded condition.
2. To simulate and visualize the flow structure over the wing for both cases (clean and loaded) as well as to obtain the lift and drag force produced from the flow field over the airfoil.

## 1.4 SCOPE OF STUDY

The simulation will be conducted using NACA 4412 airfoil as the wing sample which are oriented at an angle of attack of 0, 15, 17.5 and 20 degrees to simulate the range of angle of attacks at which the degree of flow separation is at its near maximum. In addition to the angle of attack, the simulation will also be conducted with the presence and absence of an external attachment (i.e. missile) located under the airfoil. The airfoil will also be tested under various air flow velocity to study the changes in the air flow pattern over the airfoil when the airfoil is subjected to air flow of different velocities.

# CHAPTER 2

# LITERATURE REVIEW

## 2.1 HISTORY OF AIRFOIL DEVELOPMENT

According to Kroo (2007), the development of airfoil have begun even as early as the late 1800's. Initially, it is universally recognized that a flat surface is capable of generating lift when it is subjected to fluid flow at an angle of incidence. However, certain individuals believe that a surface with a curvature, particularly ones that resemble a bird wing would produce lift more efficiently.

As a result of the assumption, many early pioneers experimented with the theory and came up with the early designs of an airfoil. One of the pioneer was H.F Phillips. According to Kroo (2007), H.F. Phillips patented a series of airfoil shapes in 1884 after testing them in one of the earliest wind tunnels in which "artificial currents of air (were) produced from induction by a steam jet in a wooden trunk or conduit".

At around the same period of time, a German engineer by the name of Otto Lilienthal also shares the same idea as H.F. Phillips, whereby Lilienthal tested his own version of airfoils after measuring the shape of bird wings. His experiments led him to his conclusion whereby the key to successful flight was wing curvature or camber. Lilienthal's airfoil designs then became the reference to which the Wright Brothers' airfoil section designs were based upon during the early 1900s, whereby the airfoil section was thin and highly cambered.

From that point of time onwards, many airfoil section designs were created as a result of trial and error which paved the way for the creation of modern airfoil designs.

## 2.2 NACA 4412 AIRFOIL

For the purpose of simulating 3 dimensional flow field over an airfoil via Computational Fluid Dynamics (CFD), the author have chosen NACA 4412 airfoil as the test subject.

According to Heffley (2007), the term "NACA 4412" was actually a 4-digit code that was used to distinguish different airfoil design shape which follows the abbreviation "NACA". According to Suckow (2009), NACA is an abbreviation that stands for the National Advisory Committee for Aeronautics. However, according to Kiaw (2009), the code are not just limited to 4-digits code since there are also the 5-digits series, 6-digit series, 7-digit series as well as the 8-digit series whereby the latter were designed to highlight more detailed aerodynamic characteristics. (Kim & Jo-Won, 2014)

The 4- digit code signifies the dimensions that make up and also distinguish the shape of a particular airfoil from one another. According to Heffley (2007), the first digit refers to the maximum camber in percent chord. Heffley (2007) also stated that the second digit is indicates the location of maximum camber along chord line (from leading edge) in tenths of chord while the third and fourth digit indicate the maximum thickness of the airfoil in percent chord. All the dimensions such as the airfoil's chord and camber are as shown in figure 2.

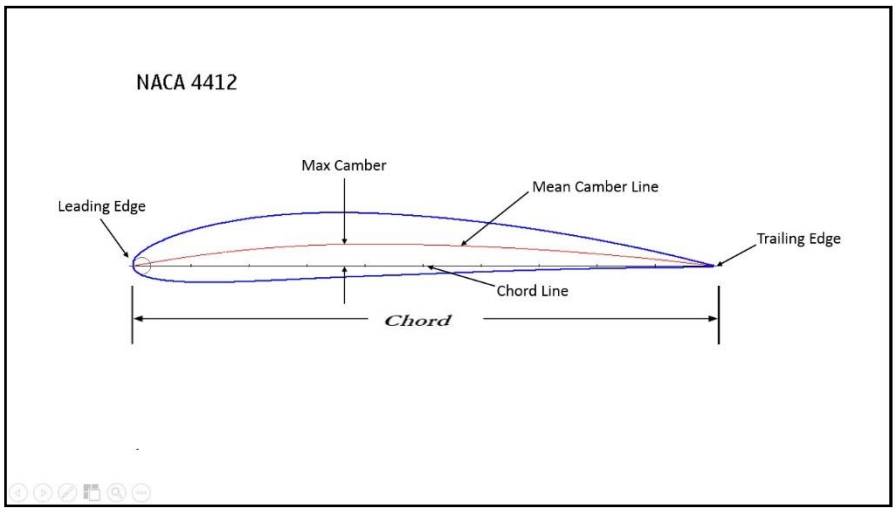


*Figure 2: Dimensions of a NACA 4412 airfoil*

## 2.3 WORKING PRINCIPLE BEHIND AIRFOILS

According to McGuigan (2014), airfoils uses the Bernoulli's principle whereby the shape of an airfoil allows wind can pass both above and below it. The shape of the top surface of the airfoil is designed in a way that as air passes over it, the air flow speeds up, therefore decreasing the air pressure in that region according to Bernoulli's principle. Air below the airfoil is not affected, so its speed is the same as it was when it first contacted the airfoil. Air with a higher pressure tends to move towards air with a lower pressure, and this difference in pressure causes force to be exerted beneath the airfoil hence generating lift.

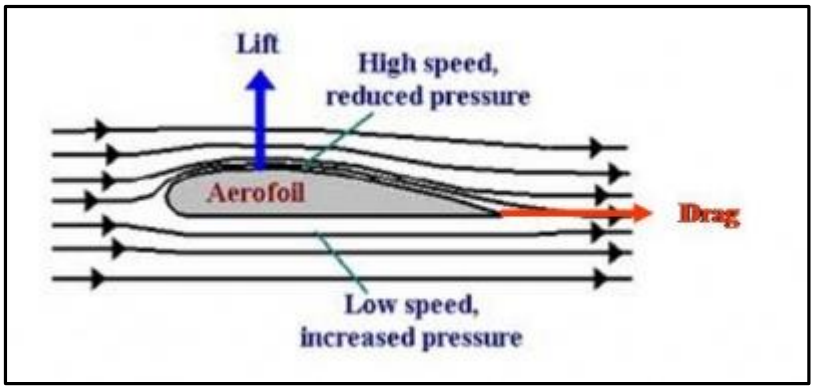


*Figure 3: Air flow around an airfoil according to Bernoulli's principle*

The equation for the lifting force that causes the airfoil to lift is as denoted by Equation 1 and Equation 2:

$F_L = C_L \times \frac{1}{2}\rho v^2 \times A$ ---------- Equation 1

$F_L = C_L \times \frac{1}{2}\rho v^2 \times (C \times L)$ ---------- Equation 2

Whereby:

C - chord length $\rho$ – density of air $v$ – velocity of air flow

L - wing span $C_L$ – lift coefficient

On the other hand, the equation for the drag that acts against the movement of an airfoil is as shown in Equation 3 and Equation 4:

$F_D = C_D \times \frac{1}{2}\rho v^2 \times A$ ---------- Equation 3

$F_D = C_D \times \frac{1}{2}\rho v^2 \times (C \times L)$ ---------- Equation 4

Whereby:

C - chord length $\rho$ – density of air $v$ – velocity of air flow

L - wing span $C_D$ – drag coefficient

# CHAPTER 3

# METHODOLOGY

In order to simulate as well as to analyze the flow field pattern around NACA 4412 airfoil in both clean and loaded condition, the author utilized a computational fluid dynamics (CFD) software as the tool to simulate and analyze the flow field pattern. Crucial parameters for the simulation as well as dimensions of the airfoil and the underwing load were determined and the simulation conducted using CFD solver to obtain all relevant results.

## 3.1 PARAMETERS AND ASSUMPTIONS FOR THE SIMULATION

There are several assumptions that were made in order to set the required variables and parameter for the simulation of flow field over clean and loaded airfoil. The assumptions and variables utilized for the simulation are as following:

- Fluid flow characteristic: Turbulent flow
- Incompressible flow
- Fluid flow velocity: 10 m/s
- Type of fluid: Air
- Fluid density: 1.225 $kg/m^3$
- Fluid viscosity: $1.7894 \times 10^{-5}$ kg/m-s
- Chord length of airfoil: 250 mm
- Airfoil span: 100 mm

## 3.2 DIMENSIONS OF NACA 4412 AIRFOIL AND AIRFOIL'S UNDERWING LOAD

The dimensions shown in Figure 4 and Figure 5 will be the geometrical measurements which will be utilized for the modelling of the 3-dimensional model of the airfoil in both clean and loaded conditions. The dimensions of both the airfoil and the under load are as following:

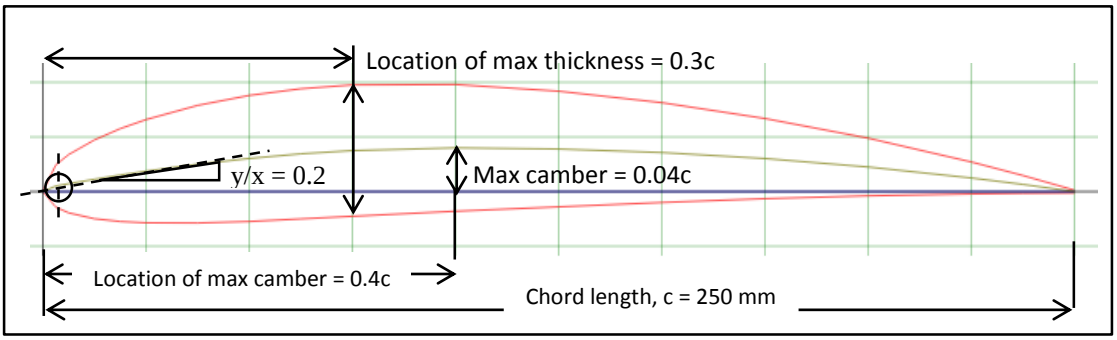


*Figure 4: Dimensions for the NACA 4412 airfoil*

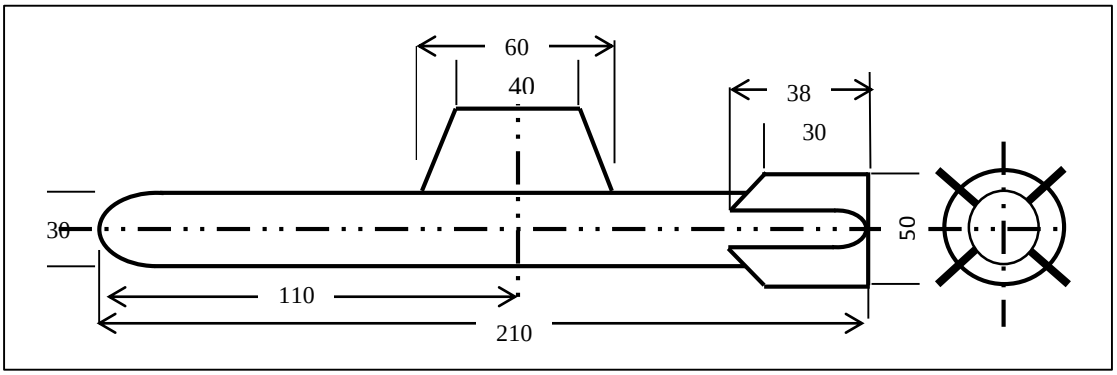


*Figure 5: Dimensions for the under load*

## 3.3 SOFTWARE USED FOR SIMULATION

For the purpose of this project which requires computational simulation of flow field over NACA 4412 airfoil, there will be no physical tools or equipment required. Computational Fluid Dynamics (CFD) software will be used to conduct all the necessary simulations. For this project, the author will be using FLUENT version 14.0 which is a CFD solver under the ANSYS group of software.

## 3.4 FLOW CHART OF SIMULATION PROCESS


*Figure 6: Flow chart for the simulation process*

## 3.5 GANTT CHART FOR THE PROJECT

| No | Detail of Work | FYP 1 | | | | | | | | | | | | | | FYP 2 | | | | | | | | | | | | | |
|---|---|---|---|---|---|---|---|---|---|---|---|---|---|---|---|---|---|---|---|---|---|---|---|---|---|---|---|---|---|
| | | 1 | 2 | 3 | 4 | 5 | 6 | 7 | 8 | 9 | 10 | 11 | 12 | 13 | 14 | 1 | 2 | 3 | 4 | 5 | 6 | 7 | 8 | 9 | 10 | 11 | 12 | 13 | 14 |
| 1 | Research about NACA 4412 airfoil | | | | | | | | | | | | | | | | | | | | | | | | | | | | |
| 2 | Research about concept of airfoil and working theory of airfoil | | | | | | | | | | | | | | | | | | | | | | | | | | | | |
| 3 | Acquisition of CFD software | | | | | | | | | | | | | | | | | | | | | | | | | | | | |
| 4 | Preliminary simulation of flow field over NACA 4412 airfoil | | | | | | | | | | | | | | | | | | | | | | | | | | | | |
| 5 | Acquisition of simulation result | | | | | | | | | | | | | | | | | | | | | | | | | | | | |
| 6 | Analysis and comparison of simulation data | | | | | | | | | | | | | | | | | | | | | | | | | | | | |
| 7 | Tabulation and organizing data for report | | | | | | | | | | | | | | | | | | | | | | | | | | | | |
| 8 | Modifications / improvisation of simulation parameter | | | | | | | | | | | | | | | | | | | | | | | | | | | | |
| 9 | Re-simulation of flow field over NACA 4412 airfoil | | | | | | | | | | | | | | | | | | | | | | | | | | | | |
| 10 | Analysis and comparison of re-simulation data | | | | | | | | | | | | | | | | | | | | | | | | | | | | |
| 11 | Preparation and submission of final report | | | | | | | | | | | | | | | | | | | | | | | | | | | | |
| 12 | Submission of final report | | | | | | | | | | | | | | | | | | | | | | | | | | | | x |

Process

x Key milestones

# CHAPTER 4

# RESULTS AND DISCUSSION

## 4.1 SOLID MODELLING OF CLEAN AND LOADED AIRFOIL

Based on the dimensions given to the author, the author conducted solid modelling to design a three dimensional model of clean and loaded NACA 4412 airfoil which will then be utilized during the simulation process. Figure 6 shows the solid model of NACA 4412 airfoil in loaded condition whereas Figure 7 shows the solid model of the airfoil in clean condition whereby there is an absence of load under the airfoil.

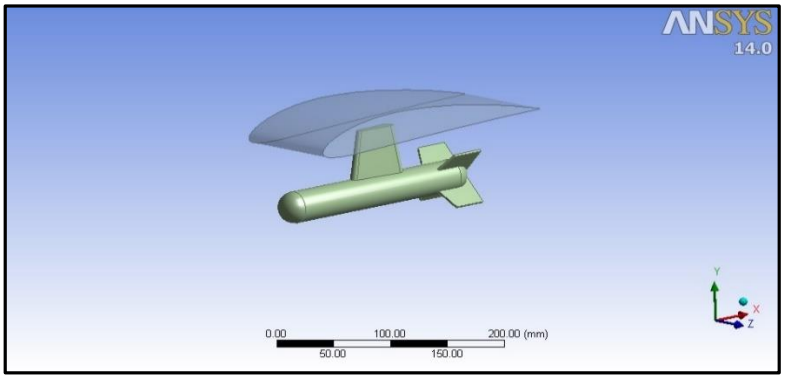


*Figure 7: 3D partial solid model of loaded airfoil section*

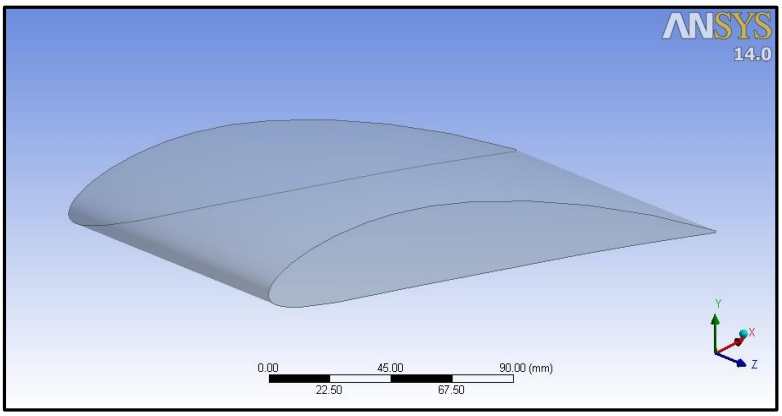


*Figure 8: 3D solid model of clean airfoil section*

The solid models shown in both diagrams above have been zoomed and enlarged in order to represent the geometry of the solid models more clearly.

## 4.2 MESHING AND BOUNDARY CONDITIONS

For the meshing process, majority the meshing perimeter are kept as per software's default with exception of the relevance center and smoothing of the meshing which are set to "medium". Besides that, relevant surfaces of the geometry are selected and named in order to distinguish the boundary of the fluid flow as well as to determine the inlet and outlet of the flow.

For the meshing process, tetrahedral mesh with patch independent setting was selected as the meshing method to produce the mesh for both clean and loaded airfoil as shown in Figure 8. For the patch independent tetrahedral meshing, several settings within the meshing method are activated such as curvature and proximity refinement setting as well as smooth transition. These settings were activated to ensure a smoother and more uniform transition between elements of different sizes within the mesh.

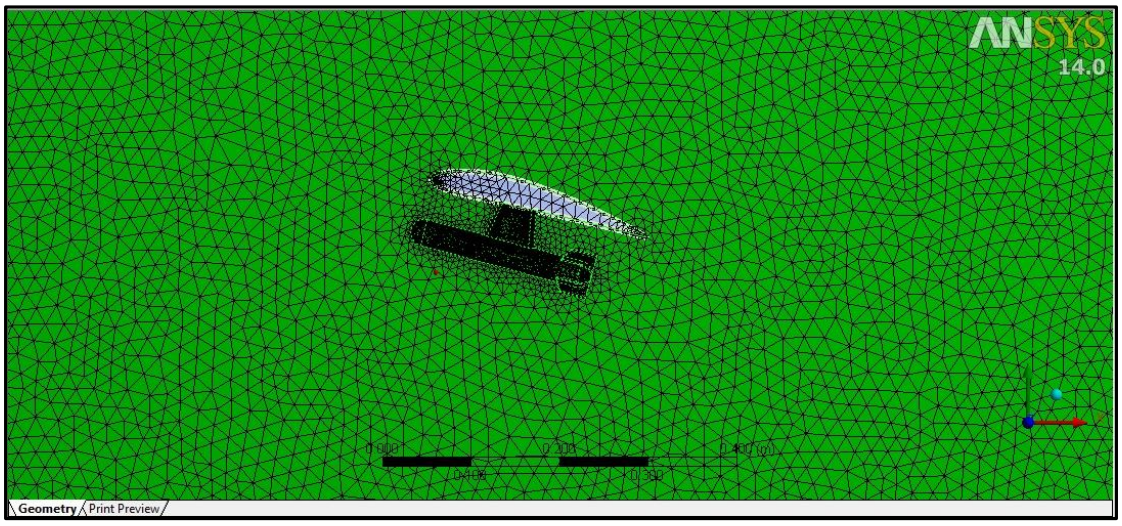


*Figure 9: Tetrahedral meshing for the loaded airfoil geometry*

For the element size of the mesh, the size of the mesh generated is 0.095102 m. The mesh element size is generated automatically by the meshing software as a result of the mesh settings chosen. After the mesh were generated, the number of nodes and elements of the mesh for both clean and loaded airfoil were observed. The number of nodes for mesh of clean and loaded airfoil ranges from 9950 nodes for clean airfoil geometry to 70875 nodes for loaded airfoil. As for the number of elements, the number of elements ranges from 46759 elements for clean airfoil geometry to 235574 elements

for loaded airfoil. The geometry of the airfoil after the meshing process are as shown in Figure 8 and Figure 9.

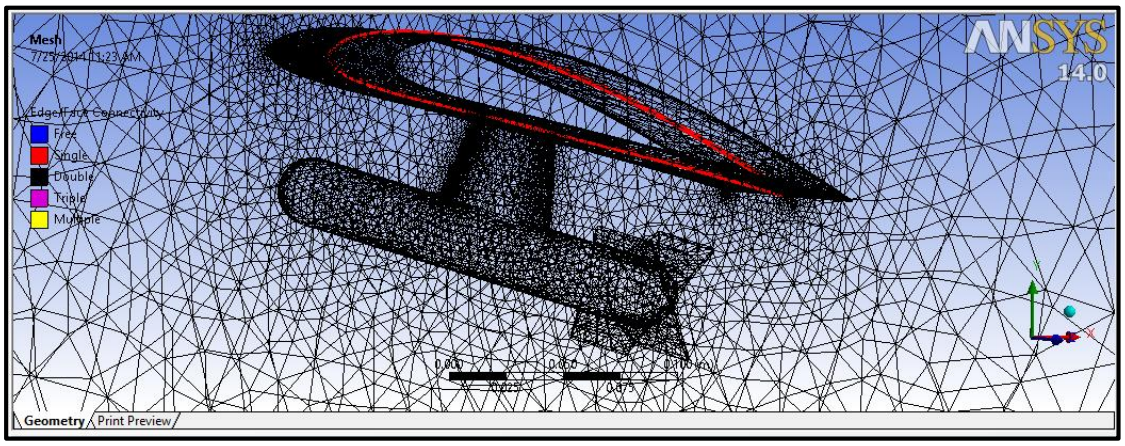


*Figure 10: Close-up of the mesh for loaded airfoil geometry*

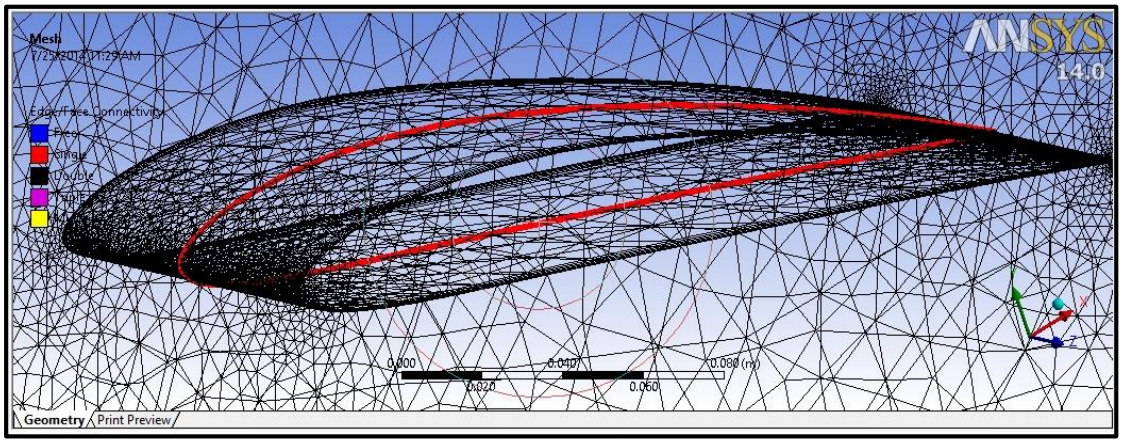


*Figure 11: Close-up of the mesh for clean airfoil geometry*

As for the boundary condition, the velocity of fluid flow at inlet is set at 10 m/s, while for the outlet, the value for pressure are set at 0 Pascal. The fluid flow model is set as laminar and the materials are set as air for the fluid volume surrounding the airfoil while the airfoil's material is set as aluminum.

## 4.3 SIMULATION RESULTS

In order to obtain visualization of the air flow field through clean and loaded airfoil, several visual method are chosen to visually demonstrate the flow field pattern. Those methods include pressure contours, velocity streamline as well as velocity vector. Apart from qualitative analysis of the flow field pattern, quantitative analysis of the simulation result are also analyzed by observing the lift and drag force acting upon the airfoil in both clean and loaded condition at different angle of attack.

### 4.3.1 CLEAN AIRFOIL AT 0 DEGREES ANGLE OF ATTACK

For the initial simulation process, the process of simulating fluid flow over clean and loaded airfoil is conducted at an angle of attack of 0 degree in which the airfoil is in a horizontal orientation and is parallel to the direction of the fluid flow. The results are obtained from simulation of both clean and loaded airfoils at 0 degree angle of attack.

Figure 11 represents the pressure contour that visually indicates the region on the surface of the airfoil with highest and lowest pressure. The result from the pressure contour indicates that there is a presence of pressure difference between the top and bottom surface of the airfoil, whereby in the diagram above, the pressure is lower near the top surface of the airfoil compared to the bottom surface of the airfoil. The presence of pressure is the crucial element that creates lift of drag force, forces which are crucial in the many field of engineering which includes aviation. The data regarding pressure can be utilized to obtain the lift and drag force acting on the airfoil.

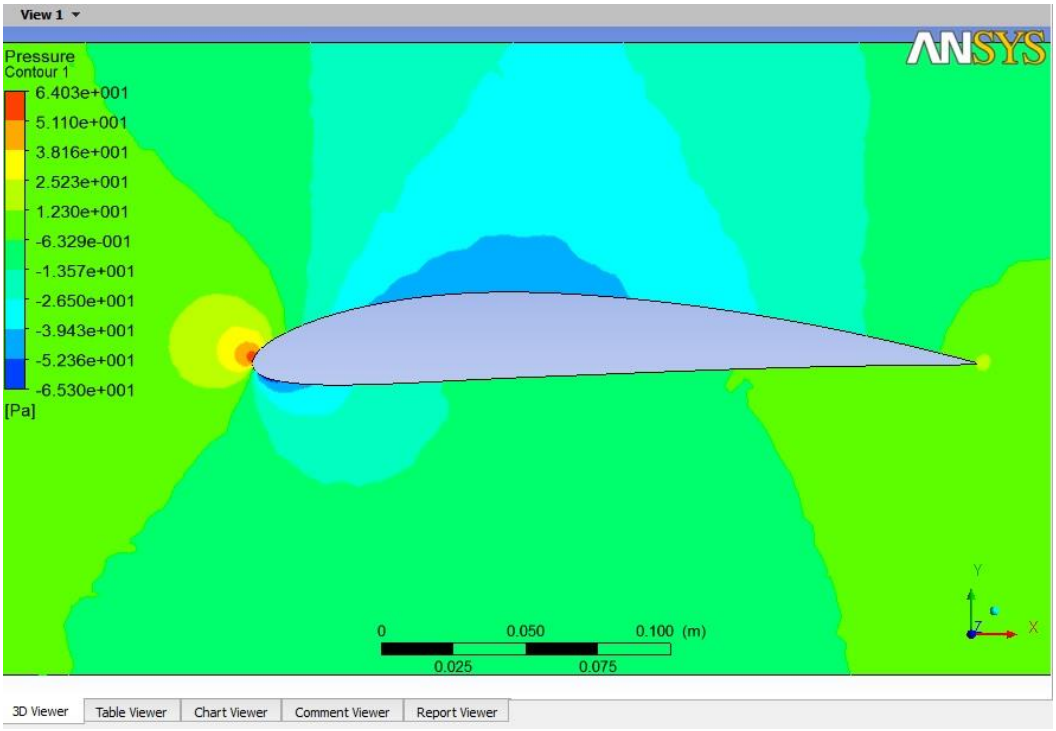


*Figure 12: Pressure contour to indicate region with highest and lowest pressure*

Figure 12 and 13 indicates the velocity magnitude of the fluid flow field over the clean airfoil via velocity streamline and velocity vector respectively. It can be observed that the velocity of fluid flow field is highest near the top surface of the airfoil as indicated by the red colored region whereas the velocity of fluid flow near the bottom surface of the airfoil is lower compared to the velocity at the top surface. Apart from that, the flow separation that occur near the surface of the wall are not too pronounced.

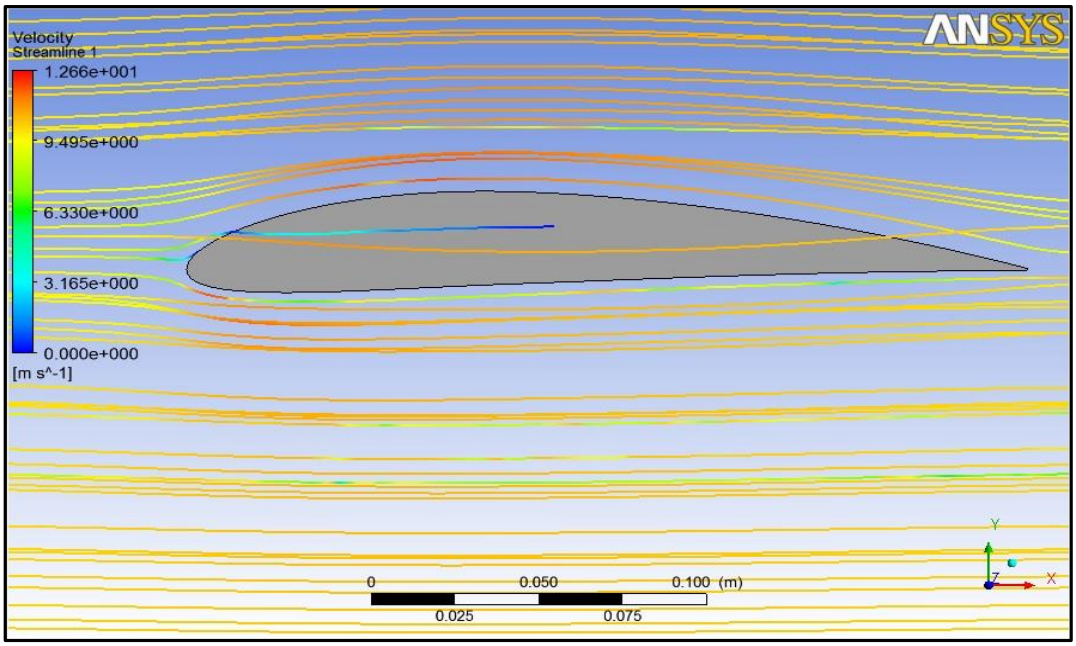


*Figure 13: Visual representation of velocity magnitude for fluid flow over airfoil via velocity streamline*

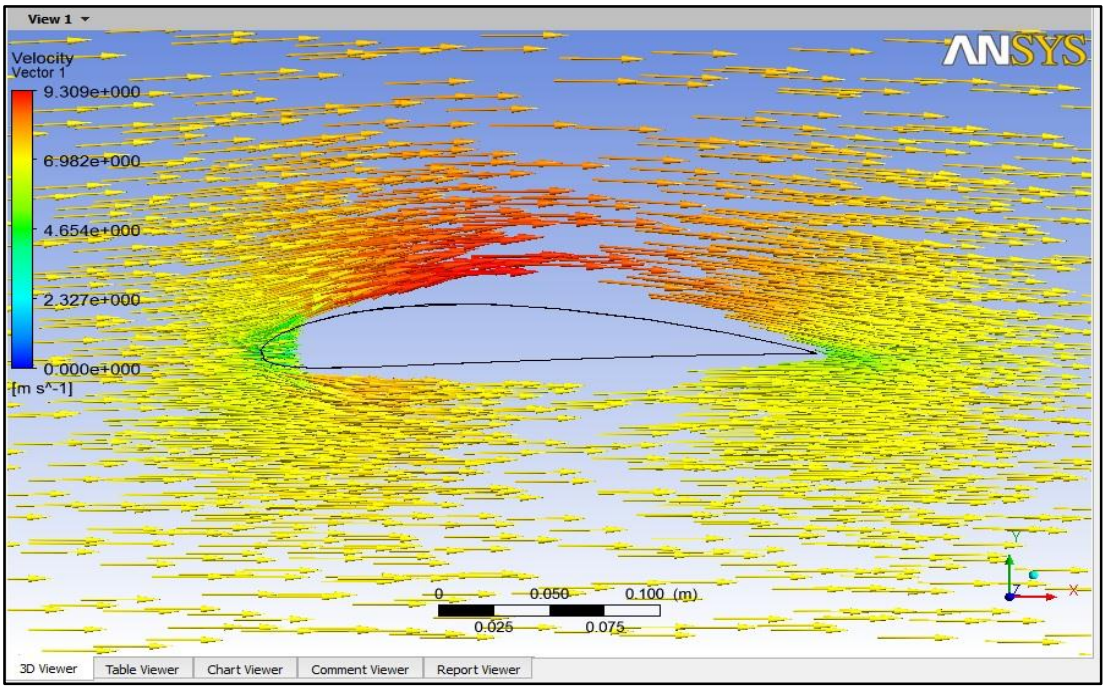


*Figure 14: Velocity vector of flow field through clean NACA 4412 airfoil at 0 degree AOA*

### 4.3.2 LOADED AIRFOIL AT 0 DEGREES ANGLE OF ATTACK

From the pressure contour diagram shown in Figure 14, it can be observed that the region with the highest pressure are located at the leading edge of the airfoil, the leading edge pylon, as well as the nose of the missile as indicated by the red colored region. Another observation that can be made is that the top surface of the airfoil have lower pressure compared to the rest of the airfoil's sections.

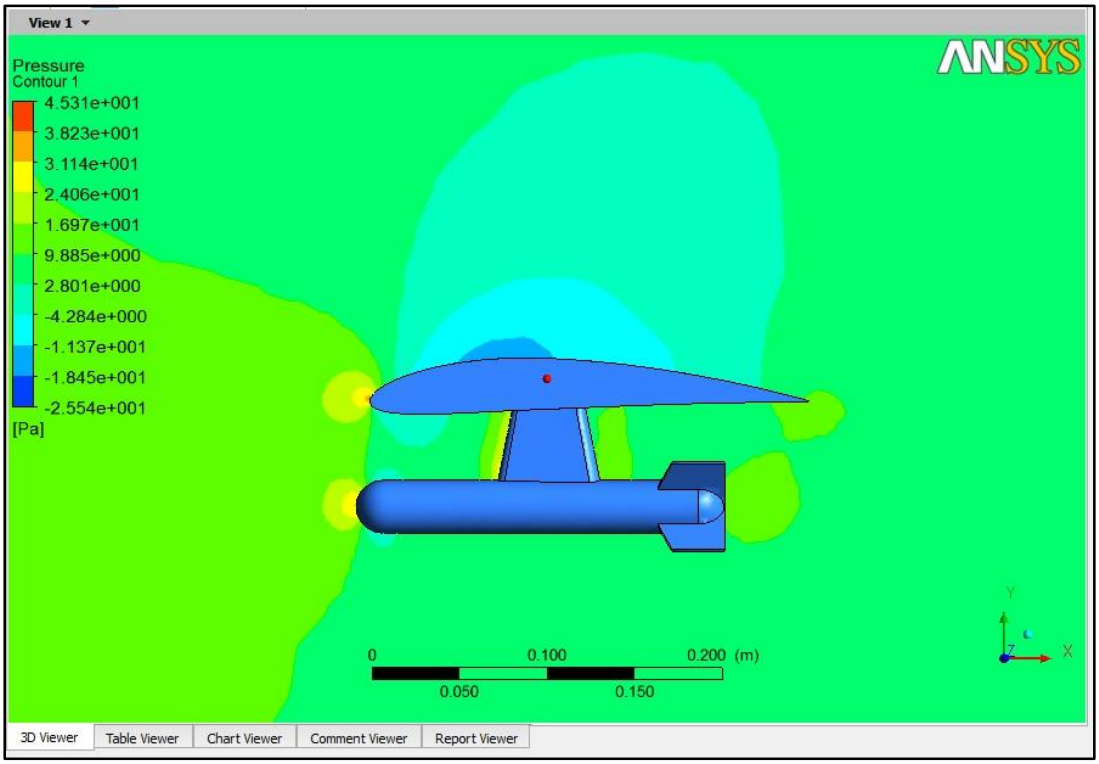


*Figure 15: Pressure contour of the loaded NACA 4412 airfoil's surface*

Figure 15 and 16 indicates the velocity magnitude of the fluid flow field over the loaded airfoil. Similar to the clean airfoil, it can be observed that the velocity of fluid flow field is highest near the top surface of the airfoil as indicated by the red colored region whereas the velocity of fluid flow near the bottom surface of the airfoil is lower compared to the velocity at the top surface.

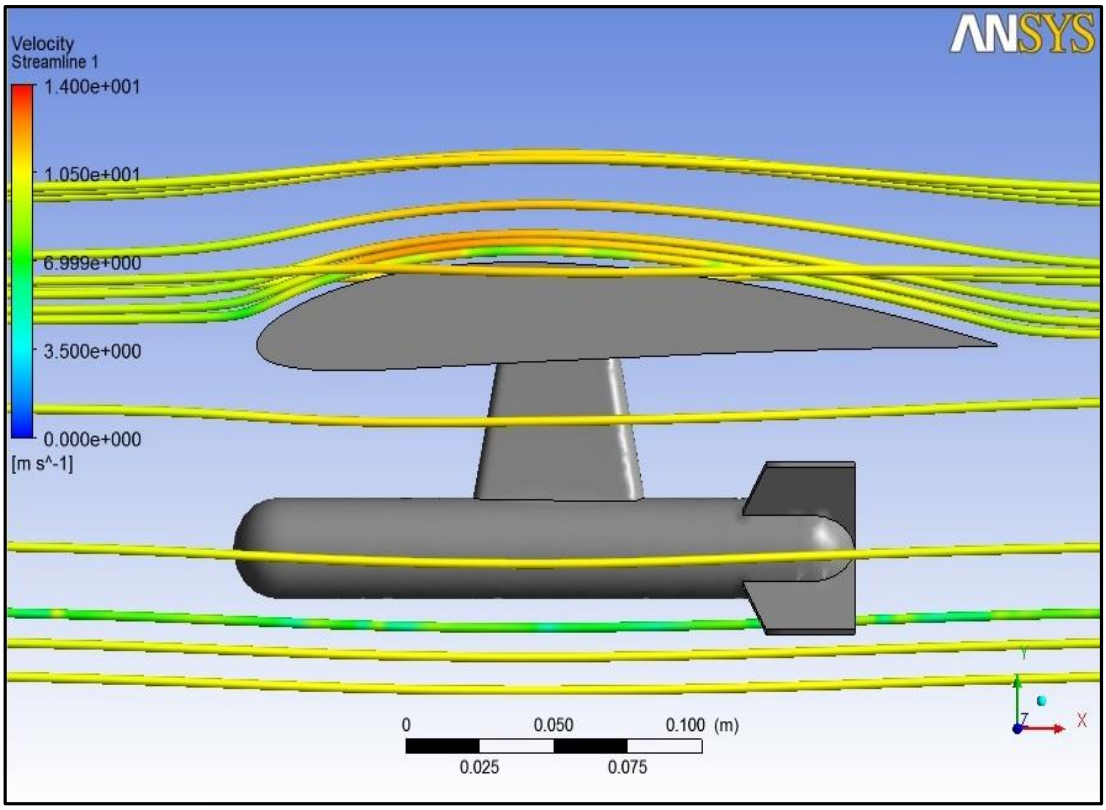


*Figure 16: Visual representation of velocity magnitude for fluid flow over loaded NACA 4412 airfoil via velocity streamline*

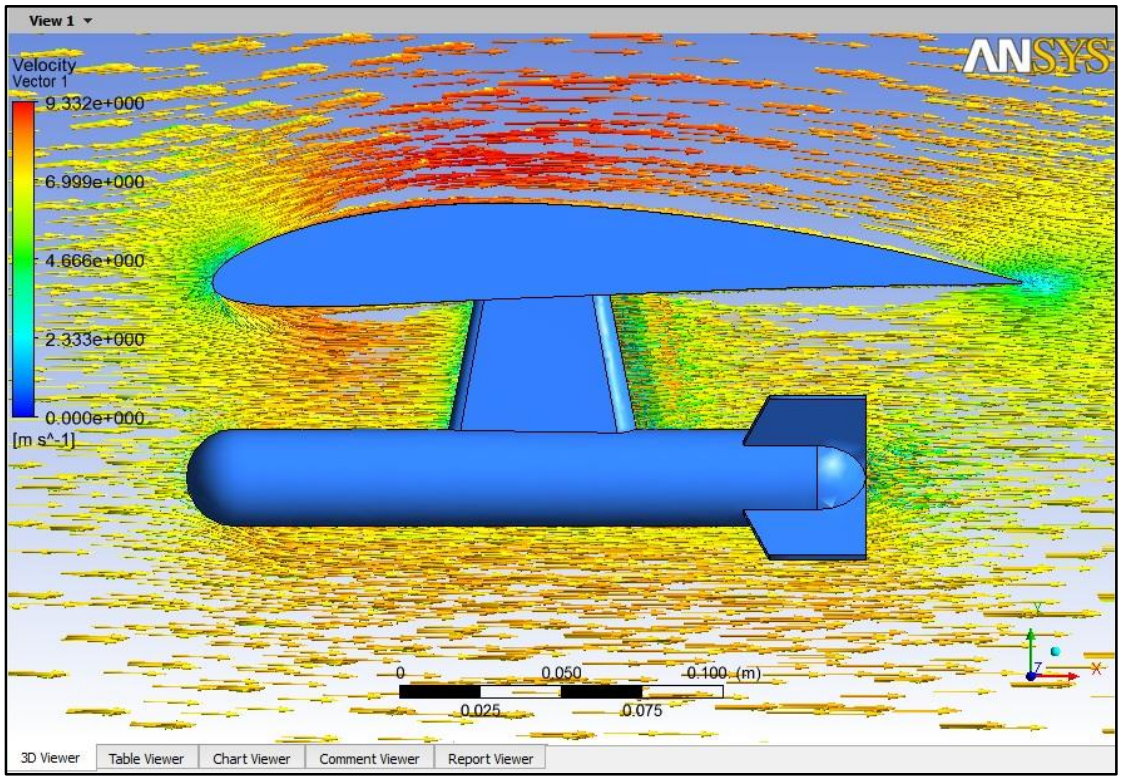


*Figure 17: Velocity vector of flow field through loaded NACA 4412 airfoil at 0 degree AOA*

### 4.3.3 CLEAN AIRFOIL AT 15 DEGREES ANGLE OF ATTACK

The diagrams below shows the pressure contour as well as velocity streamline of fluid flow through clean NACA 4412 airfoil at 15 degrees angle of attack. From the pressure contour diagram shown in Figure 17, it can be observed that the region with the highest pressure are located at the bottom surface of the airfoil, near the airfoil's leading edge as indicated by the red colored region.

Another observation that can be made is that the top surface of the airfoil in general have lower pressure compared to the bottom surface of the airfoil's section which indicate that the difference of pressure between the flow field at the bottom and top surface of the airfoil is capable of generating lift.

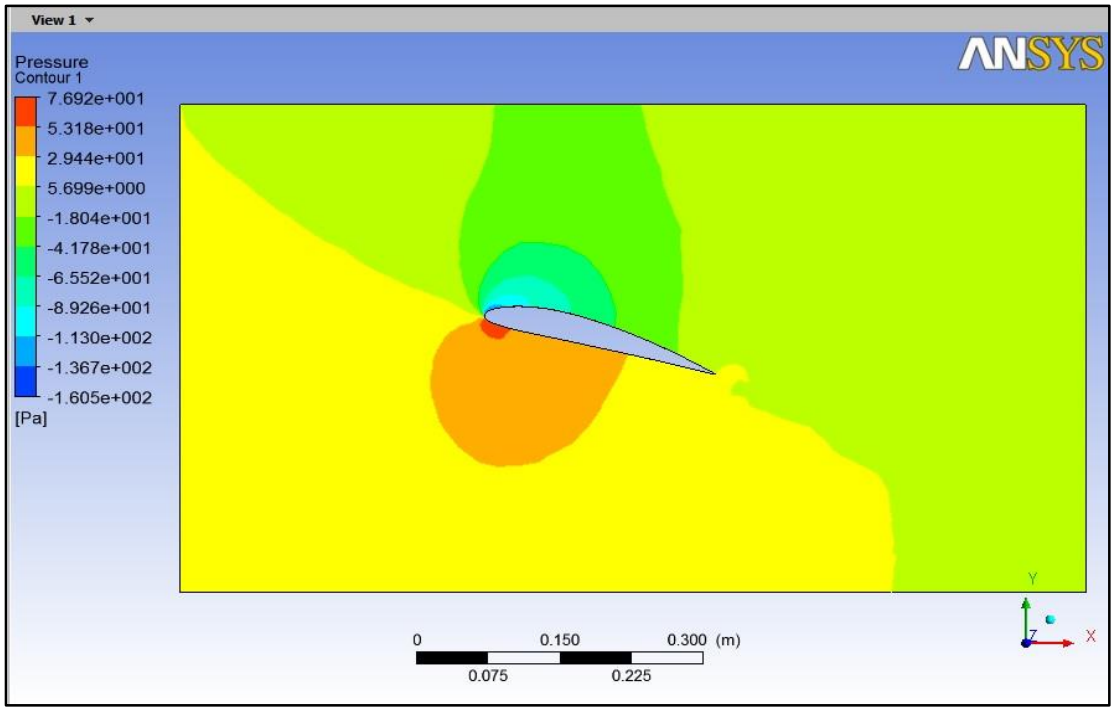


*Figure 18: Pressure contour of flow field over NACA 4412 airfoil at 15 degrees angle of attack*

As shown in Figure 18 and 19, flow separation from the flow field through clean airfoil at 15 degree angle of attack occur closer to the leading edge of the airfoil, on the top surface of the airfoil. This situation indicates that the flow separation occurs earlier on the airfoil's surface.

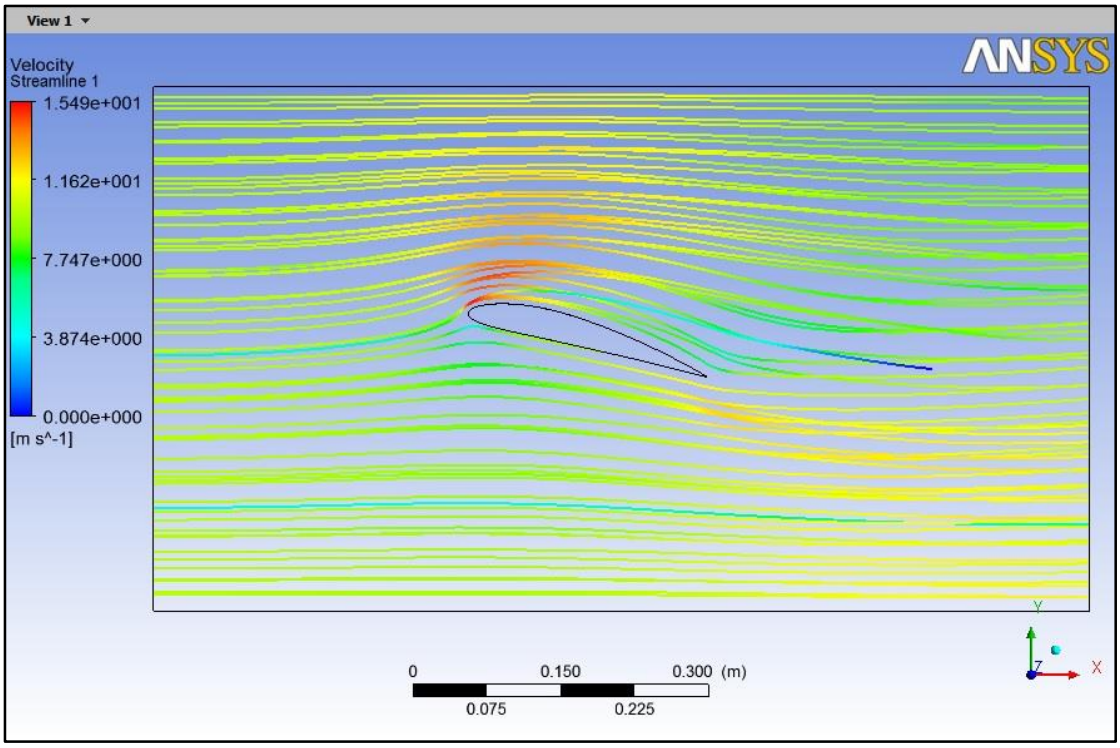


*Figure 19: Velocity streamline of flow field over NACA 4412 airfoil at 15 degrees angle of attack*

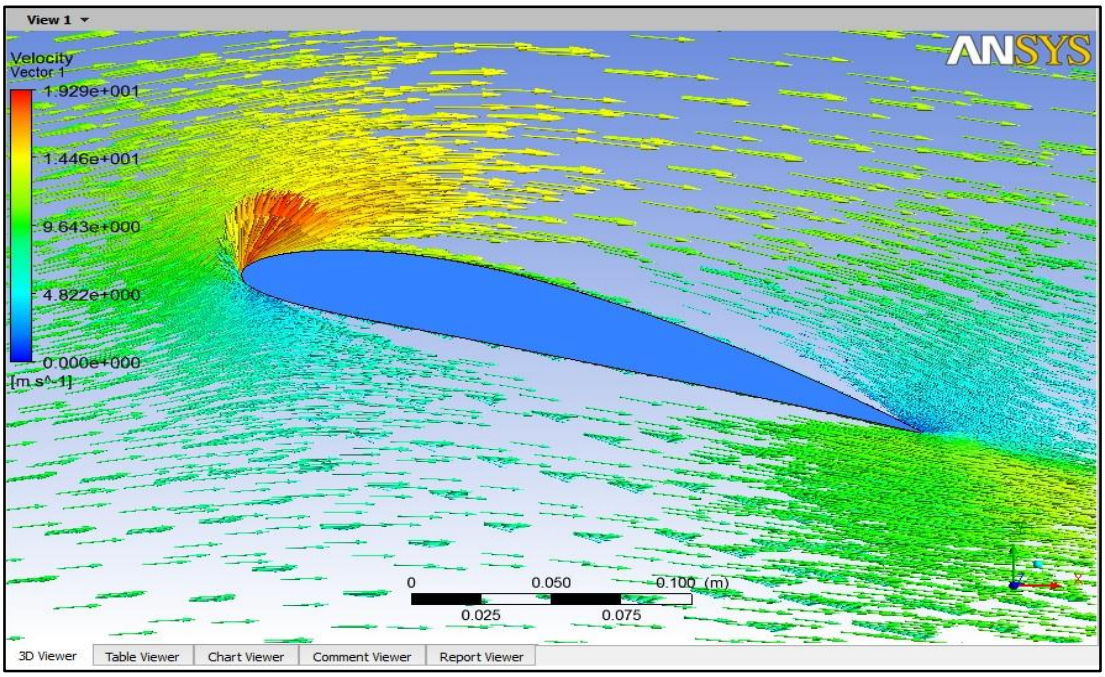


*Figure 20: Velocity vector of flow field through clean NACA 4412 airfoil at 15 degree AOA*

### 4.3.4 LOADED AIRFOIL AT 15 DEGREES ANGLE OF ATTACK

Figure 20 shows the pressure contour of the flow field through loaded NACA 4412 airfoil at 15 degrees angle of attack. It can be observed that the region with the highest pressure is located in between the bottom surface of the airfoil and the missile, as well as the nose and tail of the missile. These region of high pressure are indicated by the red colored region. On the other hand, the region with the lowest pressure is located at the top surface of the airfoil.


*Figure 21: Pressure contour of flow field over loaded NACA 4412 airfoil at 15 degrees angle of attack*

The velocity streamline in Figure 21 shows that the flow separation occurs closer towards the leading edge of the NACA 4412 airfoil compared to the airfoil at 0 degree angle of attack. The condition of the flow separation indicates that the flow separation occurs earlier on the top surface of the airfoil.

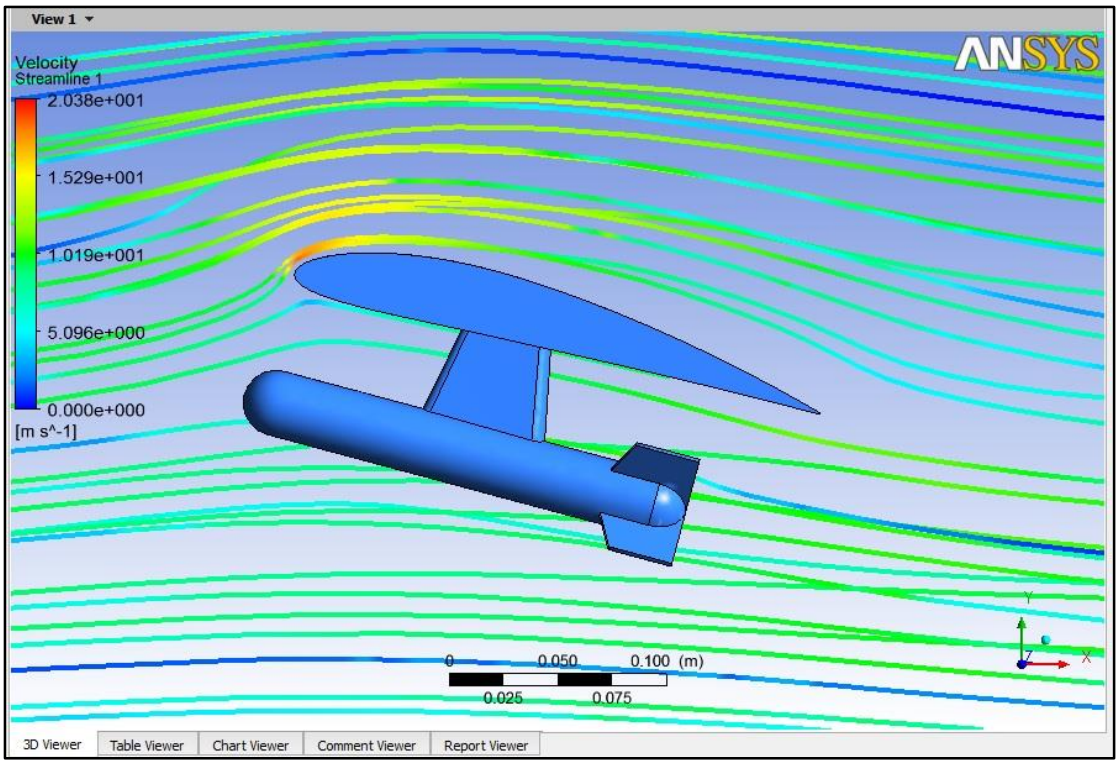


*Figure 22: Velocity streamline of flow field over loaded NACA 4412 airfoil at 15 degrees angle of attack*

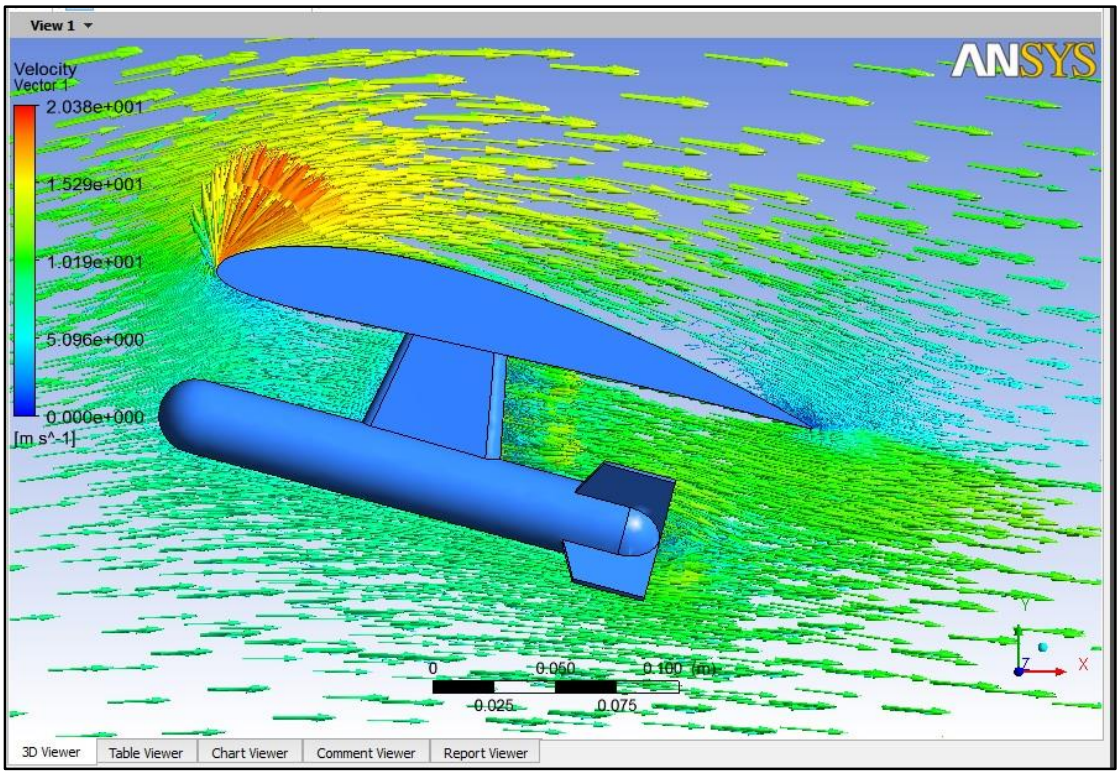


*Figure 23: Velocity vector of flow field through loaded NACA 4412 airfoil at 15 degree AOA*

### 4.3.5 CLEAN AIRFOIL AT 20 DEGREES ANGLE OF ATTACK

The diagrams below shows the pressure contour as well as velocity streamline of fluid flow through clean NACA 4412 airfoil at 20 degrees angle of attack. From the pressure contour diagram shown in Figure 23, it can be observed that the region with the highest pressure are located at the bottom surface of the airfoil. On the other hand, the region with the lowest pressure is located on the top surface of the airfoil, near the airfoil's leading edge.

Another observation that can be made is that the top surface of the airfoil in general have lower pressure compared to the bottom surface of the airfoil's section which indicate that the difference of pressure between the flow field at the bottom and top surface of the airfoil is capable of generating lift.

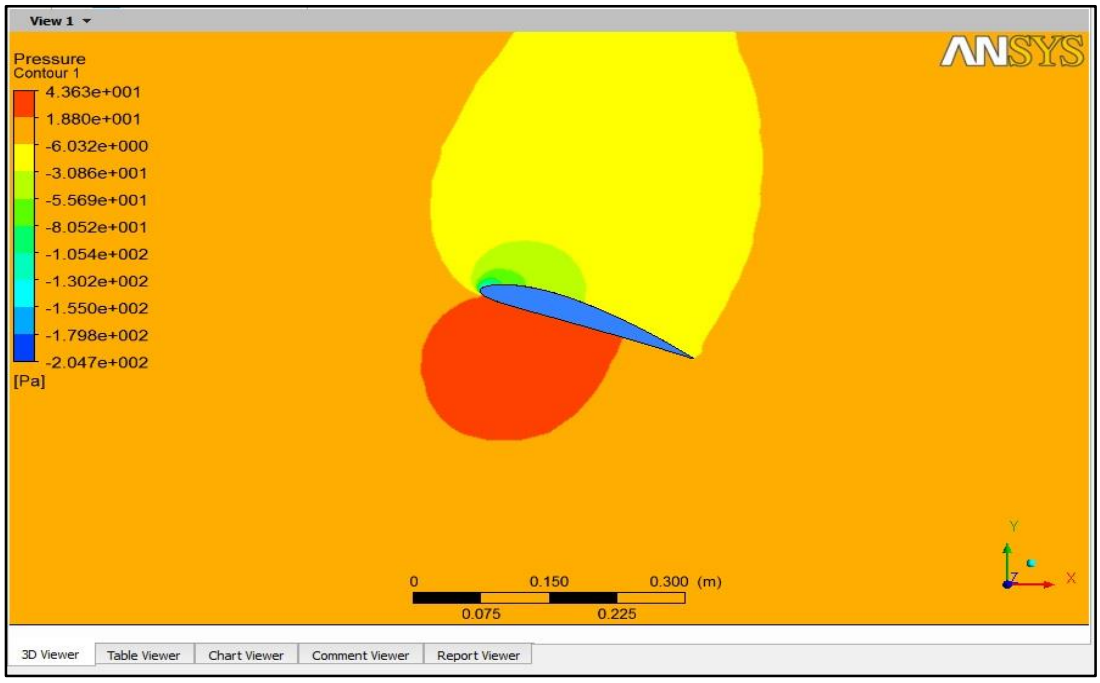


*Figure 24: Pressure contour of flow field over clean NACA 4412 airfoil at 20 degrees angle of attack*

As shown in Figure 24 and 25, flow separation from the flow field through clean airfoil at 20 degree angle of attack occur closer to the leading edge of the airfoil compared to airfoil at 0 and 15 degree angle of attack, on the top surface of the airfoil. This situation indicates that the flow separation occurs earlier on the airfoil's surface.

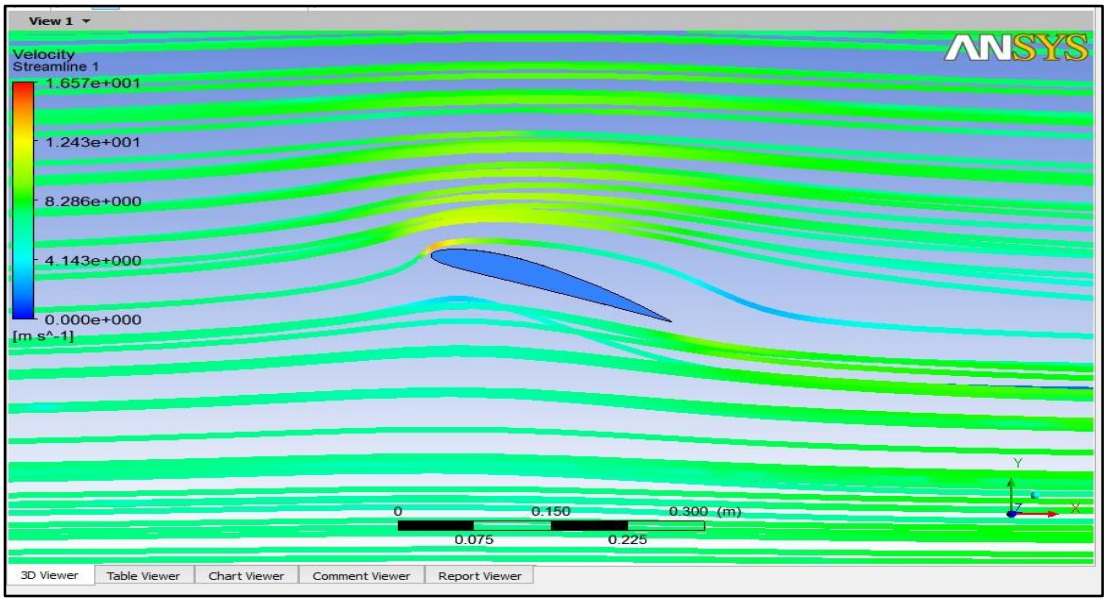


*Figure 25: Velocity streamline of flow field over clean NACA 4412 airfoil at 20 degrees angle of attack*

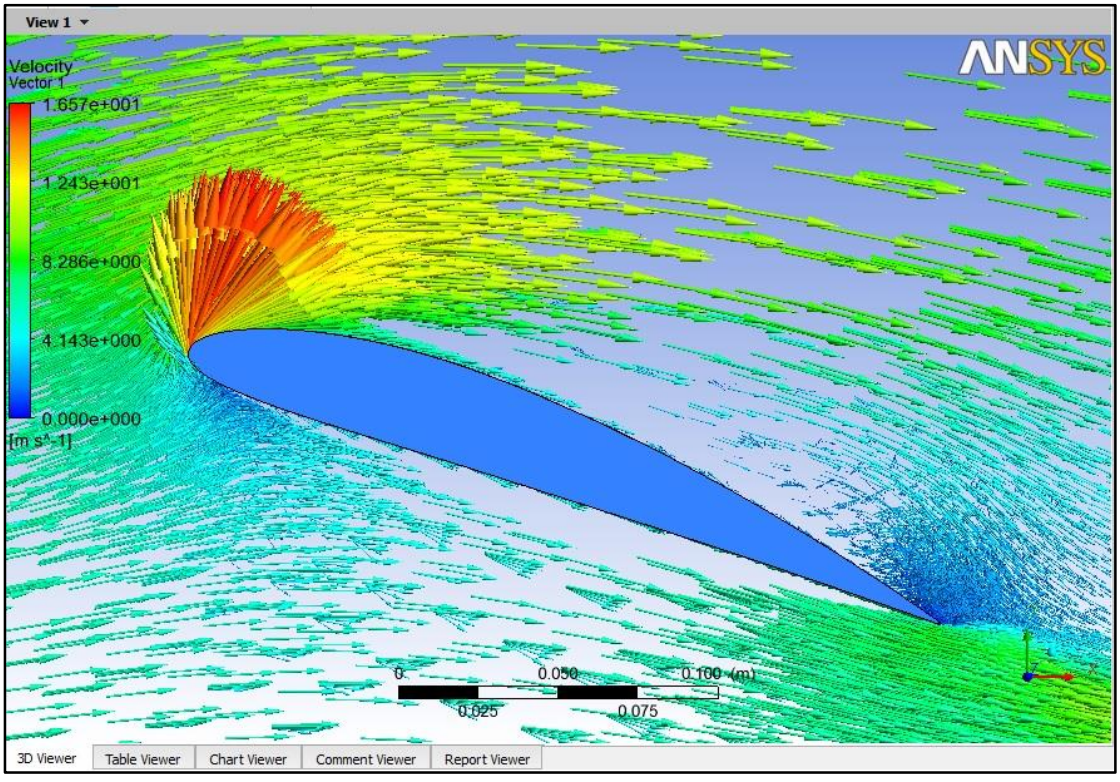


*Figure 26: Velocity vector of flow field through clean NACA 4412 airfoil at 20 degree AOA*

### 4.3.6 LOADED AIRFOIL AT 20 DEGREES ANGLE OF ATTACK

Figure 26 shows the pressure contour as well as velocity streamline of fluid flow through loaded NACA 4412 airfoil at 20 degrees angle of attack. It can be observed that the region with the highest pressure is located in between the bottom surface of the airfoil and the missile, as well as the nose and tail of the missile. These region of high pressure are indicated by the red colored region. On the other hand, the region with the lowest pressure is located at the top surface of the airfoil.

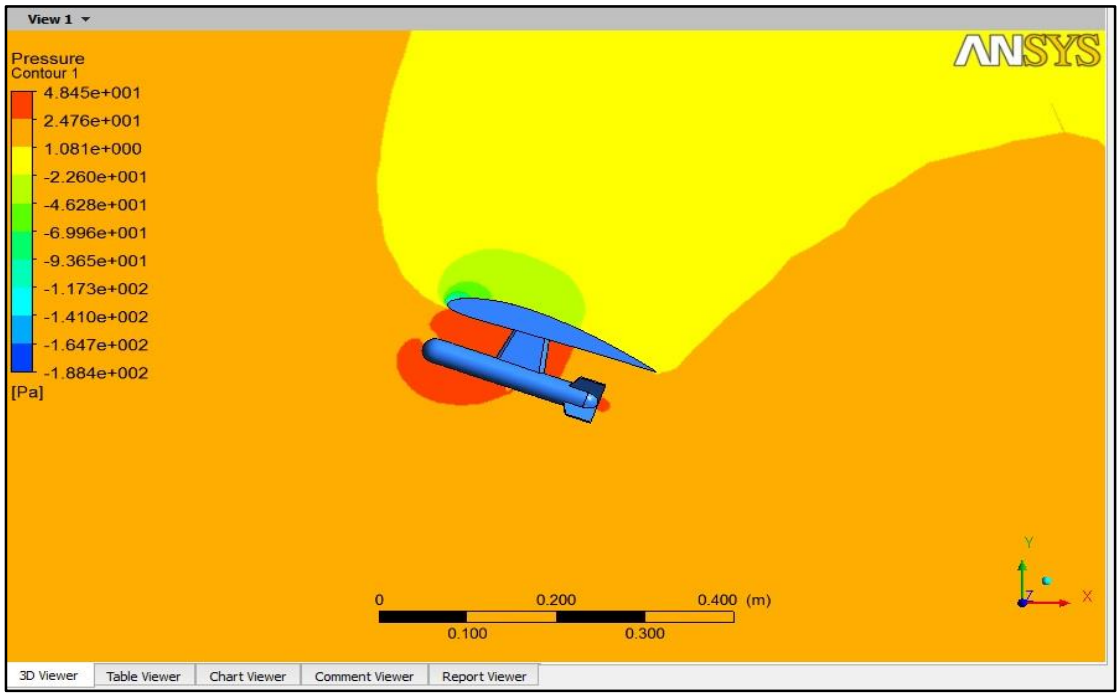


*Figure 27: Pressure contour of flow field over loaded NACA 4412 airfoil at 20 degrees angle of attack*

As indicated in Figure 27 and 28, flow separation from the flow field through clean airfoil at 20 degree angle of attack occur closer to the leading edge of the airfoil compared to loaded airfoil at 0 and 15 degree angle of attack, on the top surface of the airfoil. This situation indicates that the flow separation occurs earlier on the airfoil's surface.

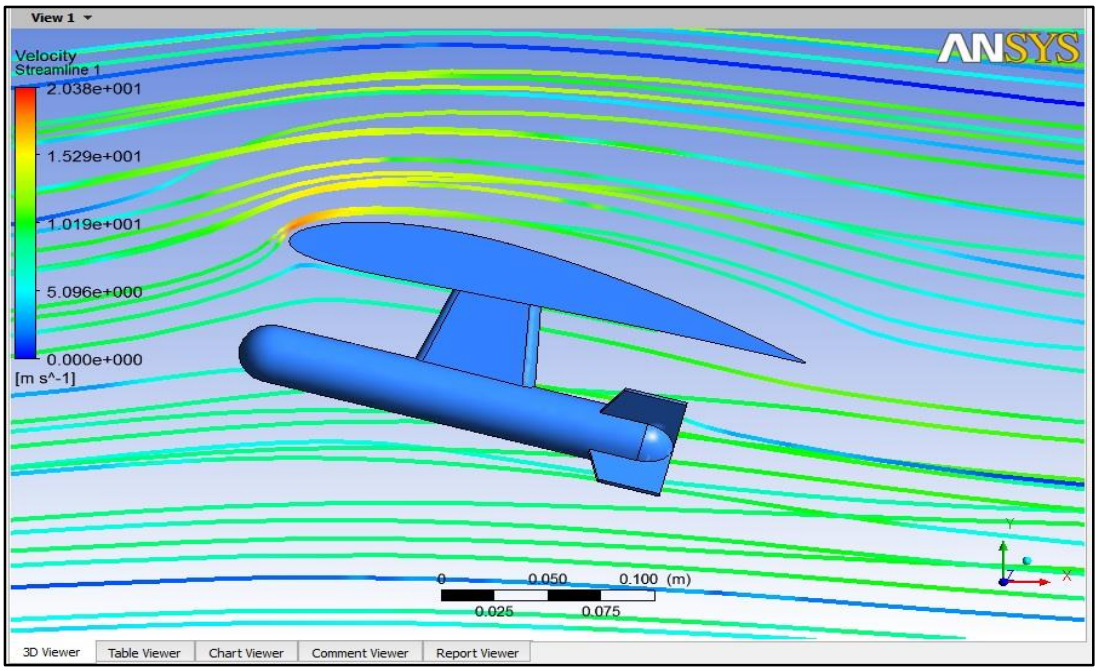


*Figure 28: Velocity streamline of flow field over loaded NACA 4412 airfoil at 20 degrees angle of attack*

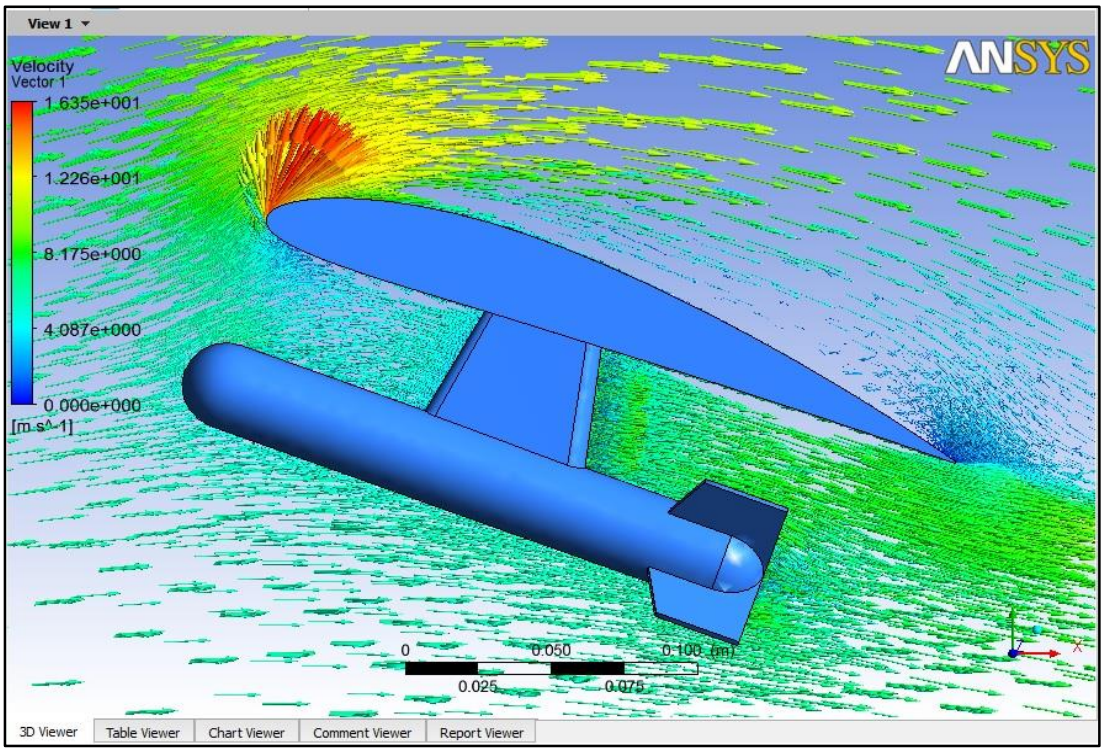


*Figure 29: Velocity vector of flow field through loaded NACA 4412 airfoil at 20 degree AOA*

### 4.3.7 LIFT AND DRAG FORCE

Apart from the qualitative data of the visualization for air flow field through clean and loaded airfoil, quantitative data obtained is the lifting force that acts upon the airfoil in order to generate lift. The lifting force generated by the fluid flow upon the scaled down NACA airfoil is obtained through the simulation process and then tabulated as shown in Table 1.

| | Force (Newton) | | Lift to drag ratio, L/D |
|---|---|---|---|
| | Lift | Drag | |
| 0 degree clean | 0.1321 | 0.0314 | 4.2070 |
| 0 degree loaded | 0.1422 | 0.0599 | 2.3739 |
| 15 degree clean | 2.4682 | 0.2880 | 8.5701 |
| 15 degree loaded | 1.1663 | 0.1433 | 8.1389 |
| 20 degree clean | 1.5336 | 0.2974 | 5.1567 |
| 20 degree loaded | 0.7314 | 0.1525 | 4.7961 |

*Table 1: Comparison of lift and drag force for clean and loaded airfoil*

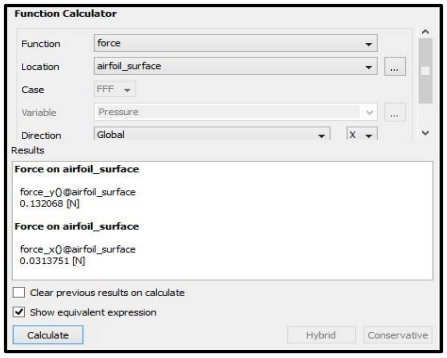


*Figure 30: Lift and drag forces obtained from the simulation for clean airfoil*

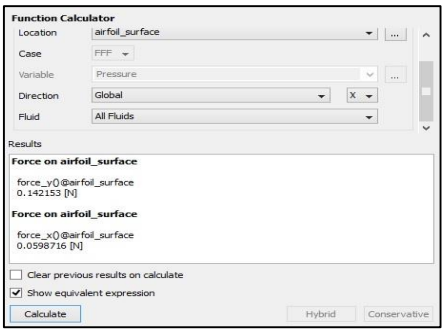


*Figure 31: Lift and drag forces obtained from the simulation for loaded airfoil*

# CHAPTER 5

# CONCLUSION AND RECOMMENDATION

In conclusion, this project is crucial as it deals with one of the essential aspect of aeronautics, which is the characteristics and pattern of air flow field generated around an airfoil, particularly the NACA 4412 airfoil which is one of the high lift airfoils family; as well as phenomenon such as flow separation of the air flow which may occur due to the angle of attack and possibly the presence of a load under the airfoil such as fairings, pods or even armaments such as missiles. The results of the simulation will complement as well as verify the data which have been obtained theoretically, and also experimentally.

One recommendation that can be implemented for the next phase of the project during Final Year Project II is by incorporating turbulence model for the simulation to simulate flow field over the clean and loaded NACA airfoil in turbulent flow field conditions.

The project is within capability of a final year student to be executed with the help and guidance from the supervisor and the coordinator. The time frame is also feasible and the project can be completed within the time allocated. It is hoped that the process of simulating the flow field over clean and loaded NACA airfoil will run smoothly and all the objectives will be achieved within the duration assigned to the author.

There are also several recommendations that can be done for future work. The recommendations include:

- To utilize more refined meshing method during the process of generating mesh for the clean and loaded airfoil geometry which may include hexahedral meshing. This meshing process will help generate a more accurate visualization of the flow field pattern, as well as the coefficient of lift and drag of the airfoil.
- To analyze the interaction between the air flow field and the airfoil at more angle of attacks.

# REFERENCES


1. Al-Kayiem, H. (2014). *Visualization of the Flow Field and wake over clean and under-loaded NACA 4412 airfoil.* Universiti Teknologi PETRONAS, Mechanical Engineering . Universiti Teknologi PETRONAS. Retrieved June 2014

2. Anandhan, P. T., & Aravindhan, P. T. (2014). Analysis of the Effects of Using Different Nozzles and Angle of Attack in Miniature Commercial Aircraft with Vertical Lift Using CFD. *Advanced Materials Research, 984 - 985*, pp. 1195-1203. doi:10.4028/www.scientific.net/AMR.984-985.1195

3. Fitzpatrick, R. (2012, April 27). *Boundary Layer Separation*. Retrieved from http://farside.ph.utexas.edu/teaching/336L/Fluidhtml/node90.html

4. *FLUENT - Flow over an Airfoil.* (2014, February). Retrieved from Cornell University: https://confluence.cornell.edu/display/SIMULATION/FLUENT+-+Flow+over+an+Airfoil

5. Gowda, B. P., & Srinivas, G. (2014, July). Aerodynamic Performance Comparison of Airfoils by Varying Angle of Attack Using Fluent and Gambit. *Applied Mechanics and Materials*, pp. 1889-1896. doi:10.4028/www.scientific.net/AMM.592-594.1889

6. Heffley, D. (2007, January 26). Retrieved from Baylor University: http://www.baylor.edu/content/services/document.php/41147.pdf

7. Kale, S. A., & Varma, R. A. (2014). Aerodynamic Design of a Horizontal Axis Micro Wind Turbine Blade Using NACA 4412 Profile. *INTERNATIONAL JOURNAL of RENEWABLE ENERGY RESEARCH, 4*(1). Retrieved 2014

8. Kale, S. A., & Varma, R. N. (2014). Aerodynamic Design of a Horizontal Axis Micro Wind Turbine Blade Using NACA 4412 Profile. *INTERNATIONAL JOURNAL of RENEWABLE ENERGY RESEARCH*, 69-72. Retrieved 2014

9. Kiaw, L. F. (2009). *AIR FLOW AROUND BODIES IN SUBSONIC WIND TUNNEL*. Durian Tunggal: Universiti Teknikal Malaysia Melaka.

10. Kim, D.-H., & Jo-WonChang. (2014, January). Low-Reynolds-Number Effect On The Aerodynamic Characteristics of a Pitching NACA 0012 Airfoil. *Aerospace Science and Technology*, *32*(1). doi:10.1016/j.ast.2013.08.018

11. Kroo, I. (2007, January). *History of Airfoil Development*. Retrieved from Applied Aerodynamics: A Digital Textbook: http://www.desktop.aero/appliedaero/preface/welcome.html

12. McGuigan, B. (2014, February 8). *What is an Airfoil?* Retrieved from WiseGEEK: http://www.wisegeek.com/what-is-an-airfoil.htm

13. Muhammad, G. F. (2010). The Effects of Cylinder AT The Leading Edge of Airfoil NACA 0012 On The Boundary Layer Separation. *Kufa journal of*

*Engineering, 1*(2). Retrieved 2014, from http://www.journals.uokufa.edu.iq/index.php/kje/article/view/2593/2212

14. Prospathopoulos, J. M., Papadakis, G., Sieros, G., Voutsinas, S. G., Chaviaropoulosm, T. K., & Diakakis, K. (2014). Assessment of the aerodynamic characteristics of thick airfoils in high Reynolds and moderate Ma numbers using CFD modeling. *Journal of Physics: Conference SeriesEmail alert RSS feed, 524*(1). doi:10.1088/1742-6596/524/1/012015

15. Qu, Q., Jia, X., Wang, W., Peiqing, L., & Agarwal, R. K. (2014). *Numerical study of the aerodynamics of a NACA 4412 airfoil in dynamic ground effect.* Elsevier. doi:10.1016/j.ast.2014.07.016

16. Richards, S., Martin, K., & Cimbala, J. M. (2011, January 17). *ANSYS Workbench Tutorial – Flow Over an Airfoil.* Retrieved from Pennsylvania State University: http://www.mne.psu.edu/cimbala/Learning/ANSYS/Workbench_Tutorial_Airfoil.pdf

17. Sharma, A., Sarwara, M. S., Singh, H., Swarup, L., & Sharma, R. K. (2014, July). CFD and Real Time Analysis of a Symmetric Airfoils. *INTERNATIONAL JOURNAL OF RESEARCH IN AERONAUTICAL AND MECHANICAL ENGINEERING, 2*(7), 84-93. Retrieved 2014

18. Suckow, E. (2009, April 21). *National Advisory Committee for Aeronautics*. Retrieved from National Aeronautics and Space Administration: http://history.nasa.gov/naca/index.html

19. Wang, S., Zhou, Y., Alam, M. M., & Yang, H. X. (2013). Turbulent Intensity Effect on Low Reynolds Number Airfoil Wake. In *Fluid-Structure-Sound Interactions and Control* (pp. 197-202). Springer Berlin Heidelberg. doi:10.1007/978-3-642-40371-2_29

20. Wray, T. J., & Agarwal, R. K. (2014). Application of New One-Equation Turbulence Model to Computations of Separated Flows. *AIAA journal, 52*(6), 1325-1330. doi:10.2514/1.J052832

21. Zhu, W. J., Shen, W. Z., & Sørensen, J. N. (2014, April 3). Integrated airfoil and blade design method for large wind turbines. *Renewable Energy*. doi:10.1016/j.renene.2014.02.057